PHYSICAL REVIEW B VOLUME 38, NUMBER 18 15 DECEMBER 1988-II

# Sequential screening layers in a photoexcited $In_{1-x}Ga_xAs/InP$ superlattice

R. E. Cavicchi, D. V. Lang, D. Gershoni, A. M. Sergent, H. Temkin, and M. B. Panish
*AT&T Bell Laboratories, Murray Hill, New Jersey 07974*
(Received 29 August 1988)

We have observed an unusual sequence of ten peaks in the derivative of the reverse-bias photocurrent in an $In_{1-x}Ga_xAs/InP$ superlattice consisting of ten wells in a *p-i-n* configuration. We show the effect is caused by the screening of the applied field by positive charge generated successively in the wells. The positive charge is a consequence of vastly different emission rates for photogenerated electrons and holes in the wells. Capacitance measurements on a *p-n* junction with a single quantum well demonstrate the effects of the different transport properties of the two carrier types. We use the quantum-confined Stark effect as an internal probe of the electric field distribution in the superlattice to confirm the model.

Multiquantum well (MQW) structures are of considerable interest, due in part to their potential device applications as photodetectors,[1] optical modulators,[2] and switches,[3] but also as model systems for studying electronic properties in semiconductors. In this Rapid Communication, we investigate the effects of differing electron and hole transport properties on the electric field distribution in a photoexcited *p-i-n* MQW structure. Passage of an electric current perpendicular to the planes of a quantum-well structure can result in the charging of individual quantum wells.[4,5] In our experiments, we show that large electric field distortions due to charging of quantum wells result from vastly different electron and hole emission rates. This is seen both for a single-quantum-well structure as well as a MQW structure.

The samples used in this work were $In_{0.53}Ga_{0.47}As/InP$ heterostructures grown by gas-source molecular-beam epitaxy. The growth technique has been described in detail elsewhere.[6] The single-well sample consisted of a $p^+$-$n$ junction with a 60-Å quantum well in the *n* region at a distance $d=4000$ Å from the junction. The MQW samples were grown on *n*-type InP ($5\times10^{17}$ cm$^{-3}$) substrates in a *p-i-n* configuration. The nonintentionally doped superlattice was prepared on a 0.25-$\mu$m-thick buffer layer and was *n* type ($5\times10^{15}$ cm$^{-3}$). The structures contained ten $In_{1-x}Ga_xAs$ 80-Å quantum wells, separated by 460-Å InP barriers. The superlattice was overgrown with a 0.3-$\mu$m-thick unintentionally doped InP layer and a 1-$\mu$m *p*-type InP ($10^{18}$ cm$^{-3}$) layer. Capacitance-voltage measurements show that beyond 2 V the depletion width is bias independent and extends across the entire superlattice and buffer regions.

We have observed in the MQW structures a series of ten peaks in the derivative of the reverse bias photocurrent, as shown in Fig. 1 for data taken at 77 K. The sample is illuminated with a 0.4-mW, 1.3-$\mu$m laser so that electron-hole pairs are only generated in the quantum wells and not in the InP. The derivative of the photocurrent is measured by applying a small ac voltage atop the dc bias and detecting the ac response with a lock-in amplifier. The peaks are periodic in voltage, with a period that depends on temperature and the intensity of photoexcitation. As the temperature is increased above 77 K, the peaks shift to lower bias, with decreased voltage separation between the peaks, and are less well resolved. Above 170 K, the number of peaks observed is reduced with increasing temperature as the peaks continue to shift to lower bias. At fixed temperature, the dependence on intensity is qualitatively similar to the dependence on temperature at fixed intensity, with reduced intensity shifting peaks to lower voltage and reducing the period. We shall argue that the peaks in the derivative of the photocurrent result from competing transport properties of holes and electrons. We will analyze this type of effect first for a single quantum well.

Consider a single quantum well in an electric field, with carriers generated at a rate *G* by photoexcitation of electron and hole pairs. The photoexcitation is at an energy below the band gap of the barriers so that the electron-hole pairs are created only in the quantum well. In a simple model for generation, recombination, and emission, the dynamics of the hole and electron populations in the well are governed by the rate equations

$$\frac{d\sigma_e}{dt}=G-\frac{\sigma_e}{\tau_e}-R\,, \quad (1a)$$

$$\frac{d\sigma_h}{dt}=G-\frac{\sigma_h}{\tau_h}-R\,, \quad (1b)$$

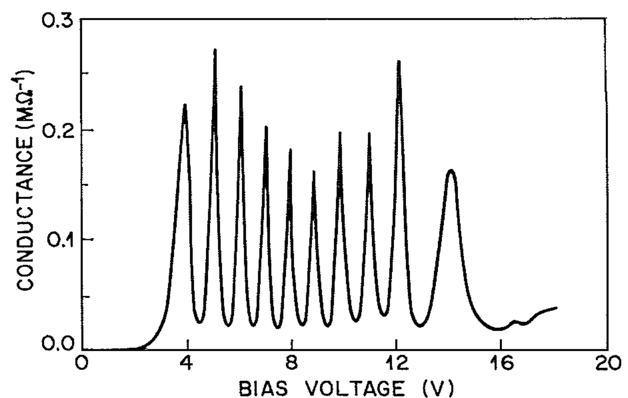


FIG. 1. Superlattice photoconductance vs reverse bias at 77 K.


©1988 The American Physical Society

where $\sigma_e$ and $\sigma_h$ are the electron and hole concentrations per unit area, $\tau_e$ and $\tau_h$ are the time constants for emission of electrons and holes, and $R$ is the recombination rate. We have investigated this case experimentally using a single-quantum-well $p^+$-$n$ diode.[7] When the diode is reverse biased to greater than 2 V, the well is in the depletion region on the $n$ side of the junction. We observe an increase in the device capacitance with the light on, which shows that photoexcitation has created an excess of positive charge in the quantum well; i.e., the quantum well acts like a giant hole trap. For an excess of holes, $R=\sigma_e/\tau_r$ where $\tau_r$ is the recombination time of an exciton. The net charge in the well $\sigma=\sigma_h-\sigma_e$ is obtained by solving Eq. (1) for the steady state,

$$\sigma=G(\tau_h-\tau_e)\tau_r/(\tau_e+\tau_r)\,. \tag{2}$$

The net positive charge shows $\tau_h > \tau_e$, an expected result, since the carrier effective mass and band offset are both larger in the valence band than in the conduction band.[8] The hole emission time may be measured by observing the capacitance transient after the light is turned off. For exciting intensities less than 0.1 mW/cm$^2$, the transient is very nearly exponential. Experiments show that above 150 K $\tau_h$ is thermally activated, while at lower temperatures it is weakly temperature dependent but depends strongly on the electric field $F$ at the well, ranging from 0.5 msec to 2 sec for $F=1.2\times10^5$–$5.6\times10^4$ V/cm. The strong field dependence is characteristic of tunneling through the triangular barrier formed by the valence-band offset and the applied plus built-in field; however, calculated times for heavy-hole tunneling yield values that are orders of magnitude too large. Hole tunneling is probably defect assisted.[9] The electron emission time $\tau_e$ is also field dependent. It may be determined from the photocurrent density $J_p$, which, using the above model, is given by

$$J_p=q\sigma_e/\tau_e=qG\tau_r/(\tau_r+\tau_e)\,, \tag{3}$$

where $q$ is the electron charge. At large reverse bias $V\sim9$ V, the photocurrent saturates at a value $J_s$ which is proportional to the excitation intensity. Saturation occurs when $\tau_e \ll \tau_r \sim 1$ nsec. At low fields, charging of the quantum well causes effects which are not included in the above model so that Eq. (3) no longer applies. A low-field value of 1 $\mu$sec is obtained from the dark frequency dependence of the admittance at zero bias when the well is occupied with electrons.[7,8]

If the photoexcitation is sufficiently intense, the net positive charge can significantly distort the electric field in the depletion region. Figure 2(a) is an energy diagram for the diode in the dark with reverse bias $V$ large enough that the quantum well is in the depletion region. In the diagram, $E_{C,V}$ are the conduction and valence bands, $\Delta E_C$ is the conduction-band offset between $In_{1-x}Ga_xAs$ and InP, $E_1$ is the lowest-lying electron state in the well, $V_{BI}$ is the built-in potential, $E_F$ is the Fermi energy in the bulk $n$-type material measured from $E_C$, and $d$ is the distance from the center of the quantum well to the $p^+$-$n$ junction. With light on, the excess of holes reduces the potential at the well. If the positive charge is large enough, the potential at the well may be reduced until $E_1$ approaches $E_F$ as shown in Fig. 2(b). When this happens electrons can

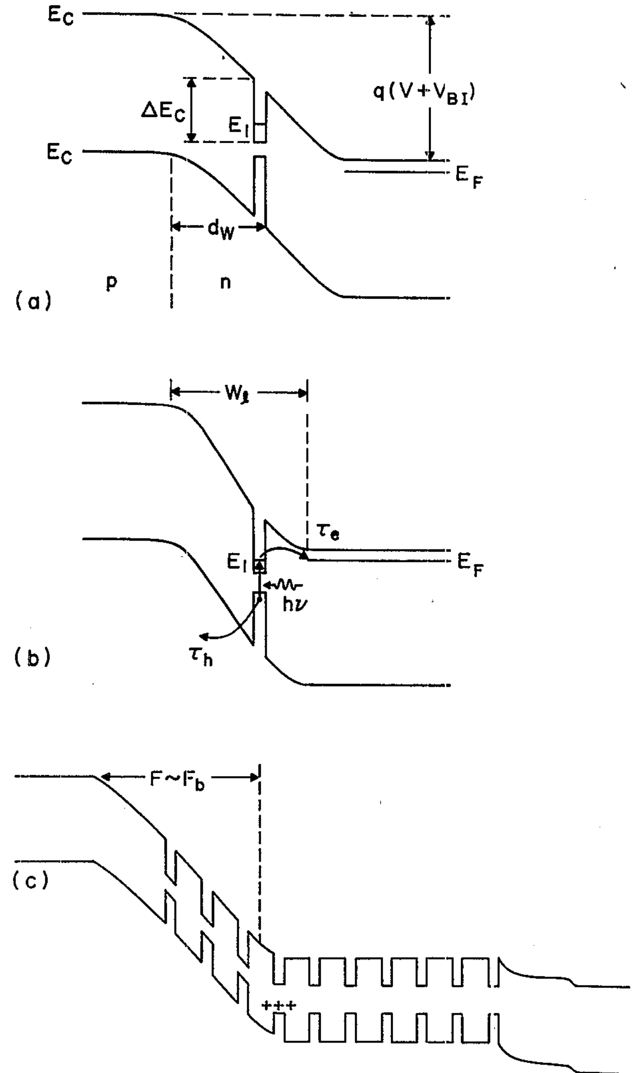


FIG. 2. (a) Band structure of quantum-well diode with reverse bias such that well is in the depletion region. (b) When illuminated, the slower emission rate of holes causes a net buildup of positive charge in the well until $E_1 \sim E_f$. (c) Band structure of illuminated superlattice; positive charge in the fourth well screens the electric field from wells further from the $p$-$n$ junction.

diffuse from the bulk into the quantum well. A dynamic equilibrium is reached where the quasi-Fermi-level in the well is aligned with $E_F$. A detailed analysis is outside the scope of this paper, but the essential consequences of the pinning of the quasi-Fermi-level can be shown by setting the quasi-Fermi-level equal to $E_1$. In this approximation, all but $\Delta E_C - E_1 + E_F$ of the voltage $V+V_{BI}$ appears between the junction and the well. The depletion width is pinned to a value $W_l$ given by

$$W_l=d+\left[\frac{2(\Delta E_C-E_1+E_F)\epsilon}{qN_D}\right]^{1/2}, \tag{4}$$

where $N_D\sim3\times10^{16}$ cm$^{-3}$ is the density of donors in the $n$-type region, and $\epsilon$ is the dielectric constant of InP. Using $\Delta E_C=0.25$ eV,[8] $E_1=75$ meV, and $E_F=-10$ meV,

calculated from the structural and doping parameters, and $\epsilon = 12.35$, we deduce $W_l \sim 5000$ Å. Figure 3 shows a set of capacitance-voltage curves taken in reverse bias on the single-well structure with varying levels of intensity. We shall express the intensity as $2.0\times10^{-\gamma}$ W cm$^{-2}$. The capacitance plateaus show the pinning of the depletion width. The depletion widths corresponding to the different capacitance plateaus at different intensities range from 5000 to 5500 Å, in reasonable agreement with our simple model. A more detailed model, which includes an analysis of the quasi-Fermi-level of electrons at different excitation intensities, should account for the different values of capacitance plateaus.

At a bias that depends on the light intensity, the single-quantum-well diode in Fig. 3 breaks away from the capacitance plateau and begins to deplete normally with increase reverse bias. This means that $\tau_h(V+V_{\rm BI})$ has been reduced by the applied field to the point that the net positive charge that can be generated by photoexcitation is insufficient to completely screen the applied field. From the difference between the light and dark capacitance, we can estimate the electric field and screening charge at a given bias by solving Poisson's equation. For example, for $\gamma=1$ at 5.6 V where the capacitance begins to drop, the electric field $F_b$ is $1\times10^5$ V/cm, and $\sigma \sim 3.5\times10^{11}$ cm$^{-2}$. We can compare this with Eq. (2), the photoexcited charge density in the absence of this Fermi-level pinning effect. At breakdown, the two values of charge density should be approximately equal. We estimate $G$ from the relation $G \approx J_s/q = 2.3\times10^{15}$ cm$^{-2}$sec$^{-1}$. The quantity $\tau_r/(\tau_e+\tau_r)$ is equal to the ratio of the photocurrent density at breakdown $J_p(V)$ to $J_s$ and is measured to be 0.25. From Eq. (2), we conclude that at the breakdown voltage for $\gamma=1$, $\tau_h \sim 0.6$ msec, a time not inconsistent with the times observed in our transient experiments at similar fields. From the experiments on the single-well sample we conclude that the slow emission rate of holes in an $In_{1-x}Ga_xAs$ quantum well can cause significant charging of the well and thereby distort the electric field in the depletion region.

The same phenomenon is responsible for the sequence of peaks in Fig. 1. In the case of a superlattice, the excess of positive charge in a well appears as a sequential process; as one well breaks down, the next well becomes the charged well. Positive charge exists principally in one well which, by screening the electric field from wells further away from the $p$-$n$ junction, divides the superlattice into high- and low-field regions. Figure 2(c) shows the potential distribution across the superlattice when the fourth well is charged. Wells that have passed into the high-field region have hole emission rates much greater than the emission rate for the well at the boundary between the two regions and, thus, contain much less positive charge than the screening well. These wells also contribute most to the photocurrent. Carriers generated in the low-field region are localized in the wells and do not contribute significantly to the photocurrent. As the bias is increased, eventually there is not enough charge generated in the fourth well to fully screen the applied field. Then the fifth well becomes positively charged, and the fourth well enters the high-field region. When this occurs, there is an increase in the photocurrent, and an associated peak in the derivative of the photocurrent.

The maximum field which the well is able to screen, the breakdown field $F_b$, is determined by the condition $F_b = q\sigma(F_b)/4\pi\epsilon$, where $\sigma(F)$ given by Eq. (2) depends on field mainly through the field dependence of $\tau_h$. The voltage of the $i$th peak is given by

$$V(i) = F_b d_i - V_{\rm BI}\,, \qquad (5)$$

where $d_i$ is the position of the $i$th well as measured from the junction. Since the wells are equally separated from one another, the peaks are uniformly spaced in voltage. The first peak at 4 V corresponds to the distance between the $p^+$-$n$ junction, which is about 4 times the interwell separation. From the interpeak voltage spacing of 1.0 V, and the superlattice period 540 Å, we estimate $F_b = 1.8\times10^5$ V/cm, a value comparable to the breakdown fields in the single-well sample.

As a test of our model for a distortion of the internal field of the superlattice, we have made use of the quantum-confined Stark effect. The effect has been seen previously in this materials system.[10] We illuminate the sample with both the 1.3-$\mu$m cw laser and chopped light from a monochromator and measure the photocurrent spectra using lock-in detection at the chopping frequency. Figure 4 shows the energy of the heavy-hole exciton peak as a function of reverse bias. Also shown is data taken

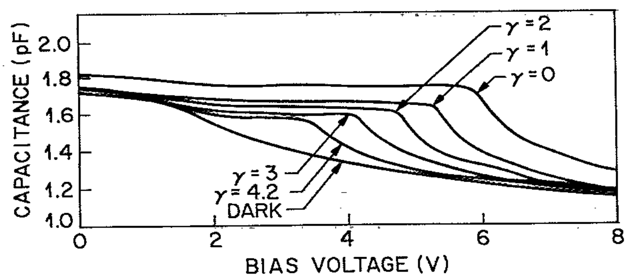


FIG. 3. Capacitance vs reverse bias for single-well diode at different intensities $I = 2.0\times10^{-\gamma}$ W cm$^{-2}$.

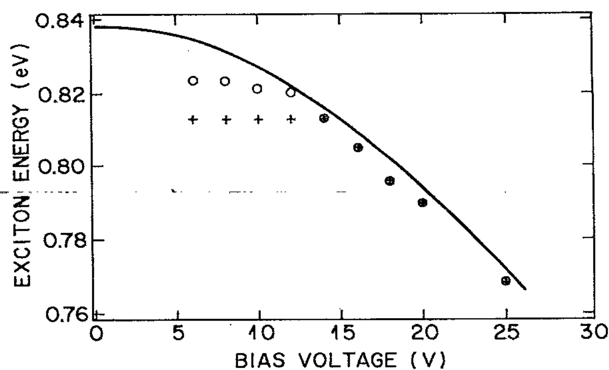


FIG. 4. Quantum-confined Stark effect in the MQW sample at 77 K. Circles are data taken with only chopped monochromator excitation; crosses are data taken with an added 0.4-mW, 1.3-$\mu$m cw laser; the curve is a calculation assuming a uniform electric field in the superlattice.

with the laser off, and a theoretical calculation of the bias dependence of the first heavy-hole exciton peak assuming a constant field in the superlattice. The energy of the heavy-hole exciton peak is bias independent in the 6–14 V range. Data in this regime are Stark shifted much more than the constant-field theory predicts. This shows that the photocurrent measured with the laser on is generated by wells in a higher field than that given by assuming a constant field. The lack of a field dependence between 6 and 14 V, indicates that wells contributing to the photocurrent are in the same electric field, independent of the bias. This is consistent with our model of wells successively entering a region of uniform field $F_b$ as they begin to contribute to the photocurrent. With the laser off, the data show that charging effects are significant even with the lower excitation intensity supplied by the monochromator. Such effects are also seen at low intensity in the single-well sample in Fig. 3. Beyond 14 V, the absorption spectra match those taken with the laser off and are in good agreement with the theory. This voltage corresponds to the last photocurrent derivative peak. Beyond this voltage, the electric field is large enough so that none of the wells contain enough charge to significantly distort the electric field. We note that at a fixed bias less than 14 V, the different absorption spectra with the laser on and off constitute a new kind of self-electro-optic effect. This effect may explain the reduced performance of quantum-well optical modulators at increased optical power levels.[11]

In conclusion, we have observed large electric field distortions in photoexcited $In_{1-x}Ga_xAs/InP$ quantum-well structures which can be understood in terms of a model using the different emission rates of photoexcited electrons and holes.

[1]H. Temkin, M. B. Panish, P. M. Petroff, R. A. Hamm, J. M. Vandenberg, and S. Sumski, Appl. Phys. Lett. **47**, 394 (1985).

[2]T. H. Wood, C. A. Burrus, D. A. B. Miller, D. S. Chemla, T. C. Damen, A. C. Gossard, and W. Wiegmann, Appl. Phys. Lett. **44**, 16 (1984).

[3]D. A. B. Miller, D. S. Chemla, T. C. Damen, T. H. Wood, C. A. Burrus, A. C. Gossard, and W. Wiegmann, IEEE J. Quantum Electron. **QE-21**, 1462 (1985).

[4]V. J. Goldman, D. C. Tsui, and J. E. Cunningham, Phys. Rev. Lett. **58**, 1256 (1987).

[5]K. K. Choi, B. F. Levine, R. J. Malik, J. Walker, and C. G. Bethea, Phys. Rev. B **35**, 4172 (1987).

[6]M. B. Panish, H. Temkin, and S. Sumski, J. Vac. Sci. Technol. B **3**, 657 (1985).

[7]R. E Cavicchi, D. V. Lang, A. M. Sergent, and M. B. Panish (unpublished).

[8]D. V. Lang, M. B. Panish, F. Capasso, J. Allam, R. A. Hamm, A. M. Sergent, and W. T. Tsang, Appl. Phys. Lett. **50**, 736 (1987).

[9]A. G. Chynoweth, W. L. Feldmann, and R. A. Logan, Phys. Rev. **121**, 684 (1961).

[10]I. Bar-Joseph, C. Klingshirn, D. A. B. Miller, D. S. Chemla, U. Koren, and B. I. Miller, Appl. Phys. Lett. **50**, 1010 (1987); and H. Temkin, D. Gershoni, and M. B. Panish, *ibid.* **50**, 1776 (1987).

[11]U. Koren, B. I. Miller, T. L. Eisenstein, R. S. Tucker, I. Bar-Joseph, and D. S. Chemla, Appl. Phys. Lett. **51**, 1132 (1987); I. Bar-Joseph, G. Sucha, D. A. B. Miller, D. S. Chemla, B. I. Miller, and U. Koren, *ibid.* **52**, 51 (1987).